Enhanced Condensation, Agglomeration, and Rejection of Water Vapor by Superhydrophobic Aligned Multiwalled Carbon Nanotube Membranes

Dokyung Yoon,[†,‡] Cheesung Lee,[†] Jongju Yun,[§] Wonjae Jeon,[§] Bong Jun Cha,[‡] and Seunghyun Baik[§,⊥,*]

[†]SKKU Advanced Institute of Nanotechnology, Sungkyunkwan University, Suwon 440-746, Republic of Korea, [‡]Research and Development Institute, Woongjin Chemical Company, Ltd., Suwon 443-270, Republic of Korea, and [§]Department of Energy Science and [⊥]School of Mechanical Engineering, Sungkyunkwan University, Suwon 440-746, Republic of Korea

ABSTRACT

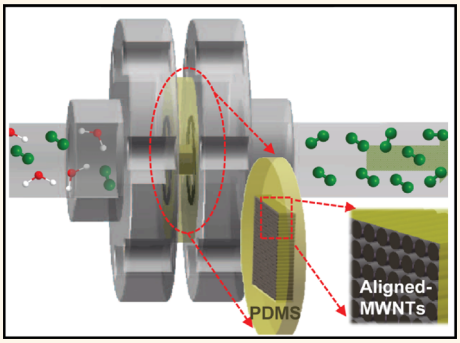

The separation of gas molecules and water vapor has become increasingly important for electronic, energy, and environmental systems. Here we demonstrate a new mechanism of enhanced condensation, agglomeration, and rejection of water vapor by superhydrophobic aligned multiwalled carbon nanotubes with the intertube distance of 73 nm, channel aspect ratio of $\sim 5.5 \times 10^4$, and tortuosity of 1.157. The array with the characteristic channel dimension some 300 times greater than the target molecule size effectively suppressed water molecular transport at room temperature with the selectivity as high as $\sim 2 \times 10^5$ (H_2/H_2O). The flow through the interstitial space of nanotubes allowed high permeability of other gas molecules (2.1×10^{-9} to 3.8×10^{-8} mol·m/m^2·s·Pa), while retaining high selectivity, which is orders of magnitude greater than the permeate flux of polymeric membranes used for the water–gas mixture separation. This new separation mechanism with high selectivity and permeate flux, enabled by the unique geometry of aligned nanotubes, can provide a low-energy and cost-effective method to control humidity.

KEYWORDS: aligned multiwalled carbon nanotube membrane · water vapor filtering · permeability · selectivity

The separation of gas and water vapor has become increasingly important in the process industry for the control of humidity,[1] removal of water vapor from natural gas,[2] and protection of electronic equipment.[3] The conventional methods of removing water vapor by hygroscopic agents or cooling the feed air below the dew point have drawbacks such as the disposal of the used agents and requirement of a large amount of energy for the gas-to-liquid phase change.[4] On the other hand, the separation process by membranes offers lower energy consumption, ease of operation, and low capital/operating costs.[1,2,5] Various polymeric membranes have been employed to selectively transport water molecules from gas mixtures.[1,6−8] Water vapor is a unique penetrant since the polar nature enables it to hydrogen bond with itself and interact strongly with the polymer, leading to the permeability in a range between 4.95×10^{-12} and 2.82×10^{-11} (mol·m/m^2·s·Pa).[1,7,8] The permeability of other gases, such as N_2, was very small (1.98×10^{-18} to 6.97×10^{-16} mol·m/m^2·s·Pa). However, the capacity and lifetime of polymeric membranes could be deteriorated by the plasticization and clustering of polymers *via* interaction with water vapor permeating through membranes.[9]

Both chemical selectivity and high flux should be achieved by the separation membranes.[10] Advances in nanotechnology enabled enhanced chemical selectivity, but it is also important to achieve high flux of permeates in spite of the significant decrease in the pore size. The flow through channel is inversely proportional to viscosity (Hagen–Poiseuille flow regime) when the characteristic channel dimension is significantly greater than the mean free path (MFP).[11] The gas separation through membranes is typically described by the Knudsen diffusion model where particle–surface collisions dominate over particle–particle collisions as the pore size becomes smaller than the MFP.[12−15] The permeability of gas

* Address correspondence to sbaik@me.skku.ac.kr.

Received for review February 27, 2012 and accepted June 19, 2012.

Published online June 25, 2012
10.1021/nn3008756

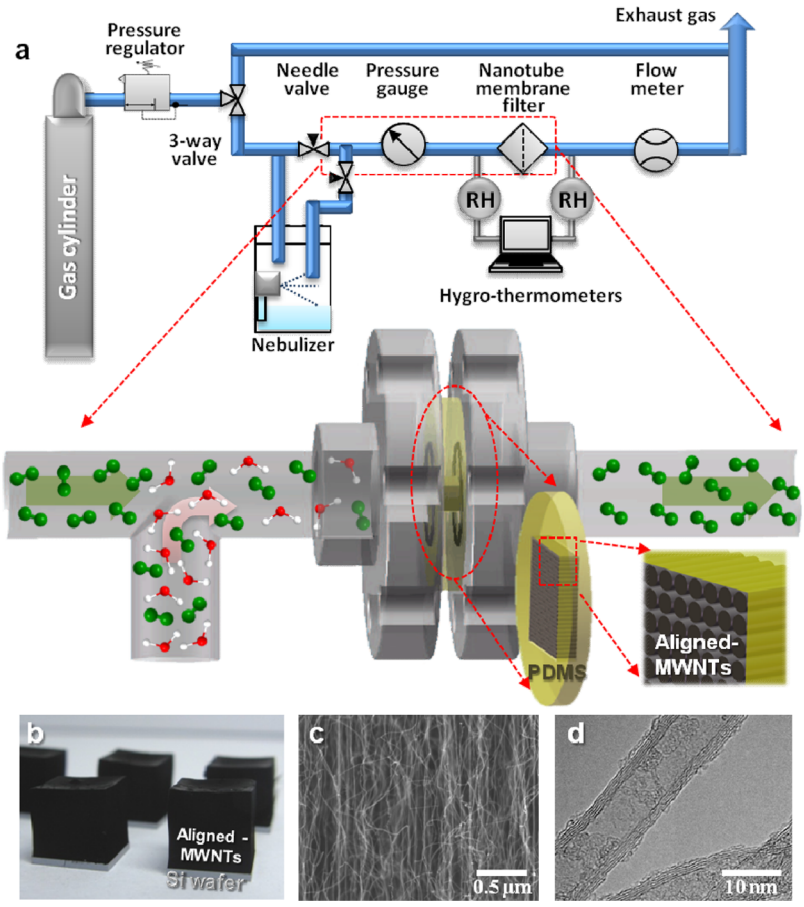

Figure 1. Gas permeability was characterized using the aligned MWNT membrane. (a) Schematic of the gas transport measurement system. The nanotube membrane and filter holder are magnified in the inset. (b–d) Optical, SEM (JEOL, JSM7500F), and TEM (JEOL, JEM2100F) images of aligned MWNTs.

molecules is proportional to the inverse square root of the molecular weight (M) in the Knudsen regime. A further decrease in the pore size comparable to that of target molecules can lead to the size exclusion by molecular sieves, resulting in a relatively small permeability of about 6.2×10^{-17} to 5.4×10^{-12} mol·m/m^2·s·Pa.[16–18]

Here we report a new mechanism to separate water vapor from gas mixtures using aligned multiwalled carbon nanotube (aligned-MWNT) membranes. The high surface roughness of the tube array induces superhydrophobicity.[19] Both theoretical and experimental works previously demonstrated the fast molecular transport through inner space as well as on the outside of nanotubes.[12,14,15,20–23] The fast permeation of water through submicrometer-thick membranes made from graphene oxide was also recently reported.[24] The interstitial space between tubes (~73 nm) was utilized in this study, without filling the gap, to maximize the flow area for high flux of permeates. The condensation of water vapor was significantly enhanced by particle–tube collisions with the channel aspect ratio of $\sim 5.5 \times 10^4$ and tortuosity of 1.157. The condensed molecules were agglomerated in the nanoscale channel, protruded out of the array, and rejected by the superhydrophobic array as will be discussed shortly. It is remarkable that the membrane with a characteristic channel dimension of 73 nm could effectively suppress the transport of water vapor. Various polar and nonpolar gas molecules were also tested, and the selectivity was as high as $\sim 2 \times 10^5$ (H_2/H_2O). The achieved permeability of single dry gases was 2.1×10^{-9} to 3.8×10^{-8} mol·m/m^2·s·Pa, which is orders of magnitude greater than the permeate flux of polymeric membranes used for water vapor separation.[1,7,8]

RESULTS AND DISCUSSION

Figure 1a shows a schematic of the gas transport measurement system. The permeability of single dry gases as well as binary mixtures was characterized using the nanotube membrane. The gas flow rate was controlled by a pressure regulator (DRASTAR Co. Ltd., DRASTAR 072), and Table 1 summarizes physical properties of gases (H_2, He, CH_4, NH_3, N_2, C_2H_4, O_2, Ar, and CO_2) used in this study.[25,26] The binary gas mixture with water vapor was generated using a nebulizer (HCT Co. Ltd., Aerosol atomizer 4810). Helium was selected as a carrier gas due to the inertness, low melting/boiling temperatures,[27] and non-adsorbing nature on carbonaceous materials.[28,29] A pressure

TABLE 1. Physical Properties of Dry Gases[a]

	MW (g/mol)	kinetic diameters (D) (Å)[25]	absolute pressure (Pa)	flow rate (sccm)	MFP (nm)	viscosity (η) (10^{-5} Pa·s)[26]	Knudsen number (K_n) of the channel	polarity (Debye)
H_2	2	2.89	163,380	21.7	67	0.88	0.9	nonpolar
He	4	2.60	163,380	21.2	83	1.97	1.1	nonpolar
CH_4	16	3.80	163,380	2.9	39	1.11	0.5	nonpolar
NH_3	17	2.60	163,380	2.3	83	0.99	1.1	1.47
N_2	28	3.64	163,380	3.0	42	1.76	0.6	nonpolar
C_2H_4	28	3.90	163,380	1.8	37	1.02	0.5	nonpolar
O_2	32	3.46	163,380	3.0	47	2.02	0.6	nonpolar
Ar	40	3.40	163,380	2.3	48	2.23	0.7	nonpolar
CO_2	44	3.30	163,380	1.2	51	1.47	0.7	nonpolar

[a] Knudsen number and MFP were calculated under the actual experimental conditions (see Supporting Information for details). The pressure on the feed side and the flow rate are also shown. The experimental conditions of He−H_2O mixtures are provided in Supporting Table S1.

sensor (DRASTAR Co. Ltd., DRA-S0030) was installed on the feed side. A flow meter with a precision needle valve (KOFLOC, RK 1200, 0.5−20 sccm) was also installed on the permeate side (see Supporting Information for details). The permeate side was at atmospheric pressure. The inner and outer diameters of the tube were 4.7 and 7.8 mm (Tygon, R-3603). The tube fittings including 2-way and 3-way valves were obtained from Sang-A Pneumatic Company (maximum air pressure ~1 MPa). The distance from the nebulizer to the nanotube membrane was 1.8 m, and the distance from the nanotube membrane to the ball flow meter was 1 m. The temperature and relative humidity (RH) on both feed and permeate sides were monitored using hygro-thermometers (TECPEL Co. Ltd., DTM-321). The capacitive-type polymer hygrometer can measure RH of a variety of gas mixtures[30] over a wide range of pressures since the saturated water vapor pressure depends only on temperature.[26] The size of a rectangular sensing element was ~3.2 × 1.4 mm^2, and the top surface was smooth, as shown in an optical microscope image (Supporting Figure S1). The experiments were carried out in a dry room at 21 °C and less than 2% RH as well as atmospheric ambient condition at ~27 °C and ~48% RH.

The aligned MWNTs were grown by thermal chemical vapor deposition,[19,31,32] and synthesis procedures are described in Methods. As shown in Figure 1b−d, the average inner and outer diameters of nanotubes were 6.7 and 10 nm with an average number of walls of 5. The nanotube length was 4 mm. The tube array (Figure 1b, 5 × 5 × 4 mm^3) was surrounded by poly(dimethylsiloxane) (PDMS) to provide a clamping area for the filter holder as shown in Figure 1a and Supporting Figure S2. PDMS did not infiltrate into the interstitial space among tubes in the central region of the array. Any attempt to open the tube ends or remove catalyst particles was not undertaken. As shown in Figure 1c, the tubes were not perfectly straight and partially entangled. The average tortuosity (τ), the degree of curviness, was 1.157 obtained using representative SEM images over the entire length of 4 mm (Supporting Figure S3).[33] The porosity, nanotube areal density, and average distance between tubes calculated based on a previously published protocol[34] were 98.5%, 1.9 × 10^{10} cm^{-2}, and 73 nm, respectively (see Supporting Information). This intertube distance is consistent with the previous reports[10] and the observation from SEM images (Supporting Figure S3). The channel aspect ratio based on the characteristic channel dimension of 73 nm and tube length of 4 mm was ~5.5 × 10^4.

Since the gap among tubes was not filled by PDMS, the molecular transport primarily occurred through the interstitial space rather than the inner holes of nanotubes. This resulted in a significantly larger flow area and higher flux of permeates. As shown in Table 1, MFP was on the same order of the characteristic channel dimension, and the Knudsen number ranged between 0.5 and 1.1. It is likely that the gas molecules collide with the tube surface at the very inlet region of the array, leading to a higher possibility of gas-to-liquid phase change of condensable molecules, such as water, as will be discussed shortly. Amorphous carbon deposits on the outer surface of nanotubes could be observed in a TEM image (Figure 1d), and there was a large D mode in the Raman spectrum of MWNTs (Supporting Figure S4a).[35] The FT-IR analysis also indicated the existence of oxygen-containing surface functional groups (Supporting Figure S4b).[36,37] This could also partly contribute to the increase in the D mode of the Raman spectrum.

Figure 2a shows the relative humidity on both feed and permeate sides monitored for more than 14 h. The experiments were carried out in a dry room at 21 °C and less than 2% RH. Four different water partial pressures were generated (30, 60, 90, and 100% RH) using He−H_2O binary gas mixtures. The relative humidity on the permeate side reached the steady state in less than 2 h, although there was somewhat of a fluctuation in the feed line due to the unstable operation of the pressure regulator and nebulizer.

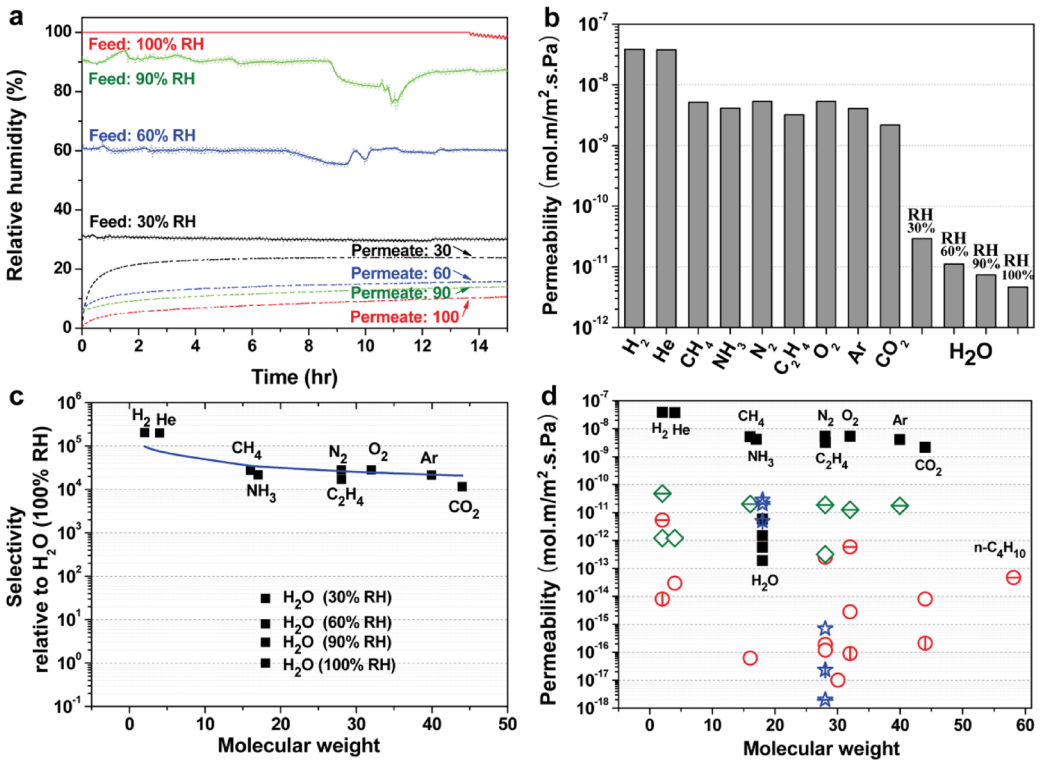

Figure 2. Gas transport through aligned MWNT membranes. (a) Relative humidity on both feed and permeate sides was monitored over 14 h. (b) Permeability of single dry gases and water vapor in binary mixtures. (c) Selectivity with respect to H_2O (100% RH). (d) Comparison of permeability. The data obtained in this study and control data from literature are shown in solid square and open symbols, respectively. ■: Aligned MWNTs. Red circles: molecular sieves.[16−18] Green diamonds: carbon nanotubes (inner holes).[14,15] Blue stars: polymeric membranes for water vapor separation.[1,7,8]

Surprisingly, the relative humidity of permeate gas mixture decreased as that of feed gas increased. The mass of filtered water was calculated using the partial pressure, temperature, volume flow rate, and psychrometric chart (Supporting Table S1). The mass of filtered water was 9.12 mg (100% RH) during the 14 h operation, whereas the increase in mass of the PDMS-surrounded aligned MWNT membrane was only 0.62 mg. We found that the mass increase in the surrounding PDMS was ~0.57 mg, due to the water absorption, in a control experiment carried out using the PDMS membrane without nanotubes. This indicates that most of the water molecules were rejected by aligned MWNTs rather than adsorption. The decreasing relative humidity of permeate with increasing relative humidity of feed gas also supports this hypothesis. The mechanism for the rejection of water molecules by the superhydrophobic aligned MWNTs will be discussed shortly (Figure 3a).

Figure 2b shows the experimentally measured permeability obtained from the volume flow rate, thickness of the membrane, flow area, and partial/total pressures (Supporting equation S22). For gas−moisture mixtures, the Dalton's assumption of ideal gas mixtures was employed to calculate the permeability of each component.[38] The partial pressure of each component was used to calculate the pressure drop, and the volume flow rate of the whole mixture was used to obtain the permeability of each component (see Supporting Information for details).[11] The permeability of water was significantly smaller than those of other polar and nonpolar gas species, and the selectivity was as high as $\sim 2 \times 10^5$ (Figure 2c, H_2/H_2O 100% RH). Three molecular transport theories through membranes (size exclusion, Hagen−Poiseuille, and Knudsen diffusion theories) were compared with the experimental data (Supporting Figure S5). None of them could explain the significantly reduced permeability of water molecules. The permeability of other gas molecules except water was roughly proportional to the inverse square root of M (Supporting Figure S5c). The trendline "$M^{-0.5}$" is also shown as a guideline to data in Figure 2c. There was no systematic trend in permeability with regard to the kinetic diameter (size exclusion) or viscosity (Hagen−Poiseuille theory).[16−18,29] The experimentally measured permeabilities were significantly greater than the predictions of Hagen−Poiseuille and Knudsen diffusion theories (Supporting Figure S5b,c). The fast transport of single dry gases (H_2, He, CH_4, N_2, O_2, and Ar) through inner holes of carbon nanotubes, compared with the Knudsen predictions, was also reported previously.[14,15]

Figure 2d compares the permeabilities obtained in this study with those of molecular sieves,[16−18] carbon nanotubes (inner hole transport),[14,15] and polymeric membranes.[1,7,8] The aligned MWNTs demonstrated

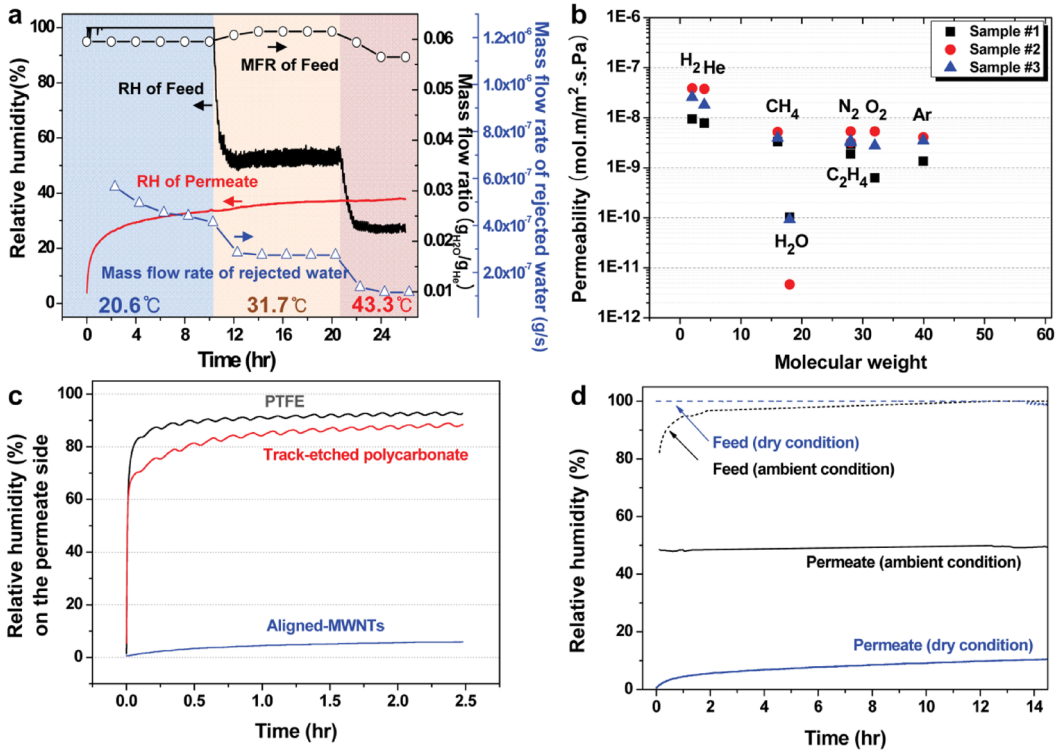

Figure 3. Mechanistic investigation of water vapor transport through aligned MWNT membranes. (a) Mass flow rate of rejected water was investigated as the feed line and membrane were heated. Three different temperatures are denoted by shaded regions (20.6, 31.7, 43.3 °C). (b) Reproducibility of three aligned MWNT membranes. (c) Comparison of water vapor transport through PTFE, track-etched polycarbonate, and aligned MWNT membranes. (d) Effect of exhaust reservoir condition on the relative humidity of permeate (dry condition, <2% RH and 21 °C, *vs* ambient condition, ~48% RH and ~27 °C).

extraordinary high permeabilities for gas species other than water. For the polymeric membranes used for water vapor separation, where the solution–diffusion theory can be applied to describe the transport phenomenon, water is a unique penetrant and other gas molecules are retarded or rejected by the membrane.[39] The permeability of water was 4.95×10^{-12} to 2.82×10^{-11} mol·m/m^2·s·Pa, whereas that of N_2 was 1.98×10^{-18} to 6.97×10^{-16} mol·m/m^2·s·Pa.[1,7,8] The flux of permeates of aligned MWNTs (gas species other than water) was 77–7800 times greater than that of permeate of polymeric membranes (water).

Figure 3a shows the change in the mass flow rate of rejected water as the feed line and membrane were locally heated by wrapping the tubing with a far-infrared flexible panel heater (Hansol DCS, Film heater C08, 15 × 80 cm^2). The relative humidity and temperature were measured using hygro-thermometers located 5 cm both upstream and downstream of the nanotube membrane. The relative humidity on the feed side decreased with increasing temperature primarily due to the increase in saturated water vapor pressure.[27] However, there was only a slight fluctuation in the mass flow rate ratio of water to He on the feed side, calculated using Supporting equations S16–S19, demonstrating the stable operation of the nebulizer. For the permeate side, the relative humidity did not show any abrupt change and the temperature was almost constant at 20.8–21.1 °C throughout the experiment. The mass flow rate of rejected water, calculated every 2 h using Supporting equation S21, decreased as the temperature of the feed line and membrane was increased. The decreased relative humidity of the feed gas and increased temperature of aligned MWNTs probably led to a decrease in the condensation of water vapor at the nanotube membrane and, therefore, a decrease in the mass flow rate of rejected water.

The following three-step mechanism (condensation, agglomeration, and rejection) is proposed for the unique filtering of water vapor by the aligned MWNT membrane. The first step is condensation. The adsorption isotherm of nanoporous carbon materials revealed energetically unfavorable adsorption of water molecules on the hydrophobic carbon nanopores due to the weak interaction.[40–44] The uptake typically initiated at relative pressures (P/P_0) of 0.4–0.6.[40,42] The cluster-mediated adsorption of water molecules was proposed since the chemical affinity of the cluster becomes less hydrophilic or even hydrophobic.[42–44] A critical cluster size of 0.6 nm, corresponding to octamers to decimers of water molecules, was suggested in carbon nanopores.[40,43] The oxygen functional groups at the surface, such as carboxyl (COOH), hydroxyl (OH), and carbonyl (C=O), can also enhance the adsorption of water molecules due to the tendency

to form hydrogen bonds.[41,42] In this work, the adsorption of water molecules would take place on top and side walls of nanotubes. The water molecules in the nanopore associate to form clusters on condensation since they cannot form large gas clusters that are larger than the pore size due to the geometrical restriction.[40] It is also possible that the surface functional groups, confirmed by the FT-IR analysis (Supporting Figure S4b), may enhance the condensation of water vapor. The continuous supply of water molecules into a membrane with a large channel aspect ratio and high molecular selectivity, such as the flow system used in this study, would increase the local concentration and relative pressure of water which is favorable for the water condensation.

The next step is agglomeration. The adsorbed molecules on the sidewall of nanotubes act as secondary nucleation centers for the cluster growth.[42] The grand canonical Monte Carlo simulation demonstrated that unit clusters (~0.7 nm) bridge each other to rapidly grow the size of aggregates.[40] In this study, the water aggregates are laterally confined by the hydrophobic nanotubes. The condensation study on hydrophobized silicon pillars showed that the surface tension keeps the aggregates reasonably spherical to grow upward and protrude above the surface of pillars.[45] The macroscopic aggregates (*i.e.*, droplets) also coalesced with another neighboring top surface droplet[46] or condensed water that remained between the pillars.[45] Considering the small gap size and high aspect ratio of aligned MWNTs, the water molecule−surface interaction, condensation, and agglomeration would take place near the tip of nanotubes, pushing the droplets above the nanotube surface. Finally, the droplets are rejected by the superhydrophobic aligned MWNTs. The nanoscale needle-like tubes combined with the low surface energy of carbon provided superhydrophobicity which could be utilized for the rejection of water even from the surfactant-aided oil−water mixtures.[19] The Cassie−Baxter wetting regime would be more appropriate, rather than the Wenzel-type surface, to describe the droplet behavior on top of aligned MWNTs considering the large aspect ratio of channels.[45,47] The droplets would easily move and fall down from the superhydrophobic surface, aided by gravity, since the tubes are aligned laterally in the current experimental design. This unique mechanism (condensation, agglomeration, and rejection) provided remarkable filtering of water molecules with a kinetic diameter of 0.265 nm by the aligned MWNT membrane with a gap size of 73 nm while maintaining high permeability of other gas molecules.

Figure 3b shows permeability measurements from three different aligned MWNT membranes demonstrating good reproducibility. The large selectivity with respect to water vapor (feed gas: 100% RH in He) could be obtained for all membranes. A control experiment without a nebulizer on the feed side and with an oil bubbler on the permeate side was also carried out at ambient conditions. The He−H_2O mixture (100% RH) was generated by introducing He gas through a cylindrical water reservoir. There was a significant decrease in RH when the He−H_2O mixture passed through the nanotube membrane, and the result was consistent with those of the experiments carried out in a dry room (see Supporting Information for details). The mechanical durability was good. Four samples out of five tested aligned MWNT membranes endured at the pressure difference of 303.4 kPa, which is the maximum generatable pressure difference in the current experimental setup (Supporting Figure S7). The area of aligned MWNTs was 5×5 mm^2. The mechanical durability may be reduced if the membrane area increases significantly. Therefore, a parallel array of nanotube membranes may be required for scale-up of the separation of water vapor.

The intertube distance of aligned MWNTs (73 nm) makes it classified as a microfiltration (MF) membrane (pore size: 50 nm to 50 μm).[48] Two polymer-based MF membranes, a hydrophilic track-etched polycarbonate membrane (Whatman #111103, pore size = 50 nm) and a hydrophobic polytetrafluoroethylene (PTFE) membrane (Advantec #J020A047A, pore size = 200 nm), were tested under the identical flow condition, as shown in Figure 3c. The permeate side relative humidities of track-etched polycarbonate and PTFE membranes were significantly greater than that of the aligned MWNT membrane. The relative humidity of feed gas was 100%. The static water contact angles and physical properties of three membranes are compared in Supporting Figure S8 and Table S2. The superhydrophobicity of the aligned MWNT membrane with a contact angle of 155° is shown. The water permeability of aligned MWNTs, compensating the difference in the thickness of membranes, was also 3−4 orders of magnitude smaller than those of polymer-based MF membranes. This demonstrates the unique and excellent behavior of condensation, aggregation, and rejection of water vapor by aligned MWNTs.

As shown in Figure 3d, the experiments were carried out in a dry room (<2% RH and 21 °C) as well as ambient conditions (~48% RH and ~27 °C) to investigate the effect of exhaust reservoir condition on the relative humidity of permeate. The surrounding chamber condition did not affect the relative humidity on the feed side since it was separated by the nanotube membrane from the permeate side. For the experiment carried out in ambient conditions, the initial relative humidity on the permeate side was 48% and remained constant over 14 h. The water vapor on the permeate side of the tube was not initially purged. This could affect the measurement since the volume flow rate was small, although the precise reason needs to be investigated further. The steady-state relative humidity

of permeate was 10.7% in the dry condition. It will be interesting to investigate the effect of different gas species, especially polar molecules, on the water condensation on the nanotube surface in the future.

CONCLUSION

In summary, the effective filtering of water vapor by the interstitial space of aligned MWNTs, whose characteristic channel dimension was some 300 times greater than the target molecule size, was demonstrated in this study. A new separation mechanism of enhanced condensation, agglomeration, and rejection of water molecules was proposed for the superhydrophobic aligned MWNT membrane. The flow through the interstitial space allowed high permeability of other gas molecules, and the selectivity was as high as $\sim 2 \times 10^5$ for H_2/H_2O (100% RH). The gas flux comparison between our membranes of the exterior of aligned MWNTs and polymeric membranes used for moisture separation from gas mixtures revealed orders of magnitude greater permeability for our membranes. The unique geometry of aligned nanotubes with the new separation mechanism could offer a facile, low-energy, and cost-effective strategy to control humidity for electronic, energy, and environmental systems.

METHODS

Synthesis of Aligned MWNTs. Aligned MWNTs were synthesized by thermal chemical vapor deposition in a horizontal quartz tube furnace with an inner diameter of 29 mm. Detailed synthesis procedures were published previously,[19,31,32] and a brief description is provided below. Sandwich-like catalyst layers, Al_2O_3 (30 nm) and Fe (1 nm), were deposited onto a SiO_2 (300 nm)−Si wafer using an e-beam evaporator. The area was 5×5 mm^2. The furnace was purged using Ar (150 sccm) for 13 min while the temperature was increased to 760 °C. In the next step, H_2 (55 sccm) and Ar (150 sccm) were supplied as etching and carrier gases for 10 min. A mixture of C_2H_4 (25 sccm), H_2 (55 sccm), and Ar (150 sccm) was then introduced into the tube furnace for 3.5 h to grow nanotubes with an average length of 4 mm. Finally, the reactor was cooled to room temperature.

The nanotube array was surrounded by PDMS to provide a clamping area for the filter holder (Supporting Figure S2). First, the array was placed at the center of a Petri dish with a diameter of 60 mm, and a mixture of prepolymer solution (PDMS, Sewang Hitech Silicon, Sylgard 184A) and curing agent (Sewang Hitech Silicon; Sylgard 184B) in a 10:1 weight ratio was poured around the tube array. The height was carefully controlled not to cover the top of the nanotubes. The aligned MWNTs surrounded by PDMS were then cured at 60 °C for 3 h followed by the detachment of the SiO_2−Si substrate. The interstitial space among tubes in the central region of the array was not blocked.

Conflict of Interest: The authors declare no competing financial interest.

Acknowledgment. This research was supported by Woongjin Chemical Co., a grant (Code No. 2011-0031635) from the Center for Advanced Soft Electronics under the Global Frontier Research Program, and WCU (World Class University) program (R31-2008-000-10029) through the National Research Foundation of Korea funded by the Ministry of Education, Science and Technology, Korea.

Supporting Information Available: Detailed synthesis procedures and additional data. This material is available free of charge *via* the Internet at http://pubs.acs.org.

REFERENCES AND NOTES

1. Mets, S. J.; van de Ven, W. J. C.; Portreck, J.; Mulder, M. H. V.; Wessling, M. Transport of Water Vapor and Inert Gas Mixtures through Highly Selective and Highly Permeable Polymer Membranes. *J. Membr. Sci.* **2005**, *251*, 29–41.
2. Baker, R. W. *Membrane Technology and Applications*; Wiley: New York, 2004.
3. Scovazzo, P.; Burgos, J.; Hoehn, A.; Todd, P. Hydrophilic Membrane-Based Humidity Control. *J. Membr. Sci.* **1998**, *149*, 69–81.
4. Zhang, L.-Z.; Wang, Y.-Y.; Wang, C.-L.; Xiang, H. Synthesis and Characterization of a PVA/LiCl Blend Membrane for Air Dehumidification. *J. Membr. Sci.* **2008**, *308*, 198–206.
5. Gebben, B. A Water Vapor-Permeable Membrane from Block Copolymers of Poly(butylenes-terephthalate) and Polyethylene Oxide. *J. Membr. Sci.* **1996**, *113*, 323–329.
6. Scovazzo, P.; Hoehn, A.; Todd, P. Membrane Porosity and Hydrophilic Membrane Based Dehumidification Performance. *J. Membr. Sci.* **2000**, *167*, 217–225.
7. Jia, L.; Xu, X. F.; Zhang, H. J.; Xu, J. P. Permeation of Nitrogen and Water Vapor through Sulfonated Polyetherethersulfone Membrane. *J. Polym. Sci., Part B: Polym. Phys.* **1997**, *35*, 2133–2140.
8. Liu, S.; Wang, F.; Chen, T. Synthesis of Poly(ether ether ketone)s with High Content of Sodium Sulfonated Groups as Gas Dehumidification Membrane Materials. *Macromol. Rapid Commun.* **2001**, *22*, 579–582.
9. Bos, A.; Punt, I. G. M.; Strathmann, H.; Wessling, M. Suppression of Gas Separation Membrane Plasticization by Homogeneous Polymer Blending. *AIChE J.* **2001**, *47*, 1088–1093.
10. Hinds, B. J.; Chopra, N.; Rantell, T.; Andrews, R.; Gavals, V.; Bachas, L. G. Aligned Multiwalled Carbon Nanotube Membranes. *Science* **2004**, *303*, 62–65.
11. Mulder, M. *Basic Principles of Membrane Technology*, 2nd ed.; Kluwer Academic: Dordrecht, The Netherlands, 1996.
12. Holt, J. K.; Park, H. G.; Wang, Y.; Stadermann, M.; Artyukhin, A. B.; Grigoropoulos, C. P.; Noy, A.; Bakajin, O. Fast Mass Transport through Sub-2-Nanometer Carbon Nanotubes. *Science* **2006**, *312*, 1034–1037.
13. Mills, A. M. *Mass Transfer*; Prentice-Hall: Upper Saddle River, NJ, 2001.
14. Mi, W.; Lin, Y. S.; Li, Y. Vertically Aligned Carbon Nanotube Membranes on Macroporous Alumina Supports. *J. Membr. Sci.* **2007**, *304*, 1–7.
15. Majumder, M.; Chopre, N.; Hinds, B. J. Mass Transport through Carbon Nanotube Membranes in Three Different Regimes: Ionic Diffusion and Gas and Liquid Flow. *ACS Nano* **2011**, *5*, 3867–3877.
16. Fuertes, A. B. Adsorption-Selective Carbon Membrane for Gas Separation. *J. Membr. Sci.* **2000**, *177*, 9–16.
17. Xu, X. Synthesis and Gas Permeation Properties of an NaA Zeolite Membrane. *Chem. Commun.* **2000**, 603–604.
18. de Vos, R. M.; Verweij, H. High-Selectivity, High-Flux Silica Membranes for Gas Separation. *Science* **1998**, *279*, 1710–1711.
19. Lee, C.; Baik, S. Vertically-Aligned Carbon Nanotube Membrane Filters with Superhydrophobicity and Superoleophilicity. *Carbon* **2010**, *48*, 2192–2197.
20. Hummer, G.; Rasaiah, J. C.; Noworyta, J. P. Water Conduction through the Hydrophobic Channel of a Carbon Nanotube. *Nature* **2001**, *414*, 188–190.

21. Kalra, A.; Garde, S.; Hummer, G. Osmotic Water Transport through Carbon Nanotube Membranes. *Proc. Natl. Acad. Sci. U.S.A.* **2003**, *100*, 10175–10180.
22. Majumder, M.; Chopra, N.; Andrews, R.; Hinds, B. J. Nanoscale Hydrodynamics: Enhanced Flow in Carbon Nanotubes. *Nature* **2005**, *438*, 44.
23. Yu, M.; Funke, H. H.; Falconer, J. L.; Noble, R. D. High Density, Vertically-Aligned Carbon Nanotube Membranes. *Nano Lett.* **2009**, *9*, 225–229.
24. Nair, R. R.; Wu, H. A.; Jayaram, P. N.; Grigorieva, I. V.; Geim, A. K. Unimpeded Permeation of Water through Helium-Leak-Tight Graphene-Based Membranes. *Science* **2012**, *335*, 442–444.
25. Breck, W. B. *Zeolite Molecular Sieves*; Wiley: New York, 1974.
26. Geankoplis, C. J. *Transport Processes and Separation. Process Principles*. 4th ed.; Prentice Hall: New York, 2003.
27. Sonntag, R. E.; Borgnakke, C.; Wylen, G. J. V. *Fundamentals of Thermodynamics*, 5th ed.; Wiley: New York, 1998.
28. Ash, R.; Baker, R. W.; Barrer, R. M. Sorption and Surface Flow in Graphitized Carbon Membranes. I. The Steady State. *Proc. R. Soc. A* **1967**, *299*, 434–454.
29. Cussler, E. L. *Diffusion: Mass Transfer in Fluid Systems*, 3rd ed.; Cambridge University: New York, 2009.
30. Chen, Z.; Lu, C. Humidity Sensors: A Review of Materials and Mechanisms. *Sens. Lett.* **2005**, *3*, 274–295.
31. Kim, H.; Chun, K.-Y.; Choi, J.; Kim, Y.; Baik, S. Effects of Catalyst on the Super-Growth of Multi-Walled Carbon Nanotubes. *J. Nanosci. Nanotechnol.* **2010**, *10*, 3362–3365.
32. Kim, H.; Lee, C.; Choi, J.; Chun, K.-Y.; Kim, Y.; Baik, S. Effects of a Sandwich-like Catalyst on the Vertical Growth of Carbon Nanotubes Synthesized by Using Chemical Vapor Deposition. *J. Korean Phys. Soc.* **2009**, *54*, 1006–1010.
33. Zhang, Q.; Zhou, W.; Qian, W.; Xiang, R.; Huang, J.; Wang, D.; Wei, F. Synchronous Growth of Vertically Aligned Carbon Nanotubes with Pristine Stress in the Heterogeneous Catalysis Process. *J. Phys. Chem. C* **2007**, *111*, 14638–14643.
34. Laurent, C.; Flahaut, E.; Peigney, A. The Weight and Density of Carbon Nanotubes *versus* the Number of Walls and Diameter. *Carbon* **2010**, *48*, 2989–2999.
35. Antunes, E. F.; Lobo, A. O.; Corat, E. J.; Trava-Airoldi, V. J. Influence of Diameter in the Raman Spectra of Aligned Multi-Walled Carbon Nanotubes. *Carbon* **2007**, *45*, 913–921.
36. Yang, D.; Guo, G.; Hu, J.; Wang, C.; Jiang, D. Hydrothermal Treatment to Prepare Hydroxyl Group Modified Multi-Walled Carbon Nanotubes. *J. Mater. Chem.* **2008**, *18*, 350–354.
37. Smith, J. G. *Organic Chemistry*, 2nd ed.; McGraw-Hill: New York, 2008.
38. Cengel, Y. A.; Boles, M. A. *Thermodynamics: An Engineering Approach*, 5th ed.; McGraw-Hill: New York, 2006.
39. Feng, H.; Zhang, H.; Xu, L. Polymeric Membranes for Natural Gas Conditioning. *Energy Sources, Part A* **2007**, *29*, 1269–1278.
40. Ohba, T.; Kanoh, H.; Kaneko, K. Water Cluster Growth in Hydrophobic Solid Nanospaces. *Chem.—Eur. J.* **2005**, *11*, 4890–4894.
41. Lee, W. H.; Reucroft, P. J. Vapor Adsorption on Coal- and Wood-Based Chemically Activated Carbons: (I) Surface Oxidation States and Adsorption of H_2O. *Carbon* **1999**, *37*, 7–14.
42. Bekyarova, E.; Hanzawa, Y.; Kaneko, K.; Silvestre-Albero, J.; Sepulveda-Escribano, A.; Rodriguez-Reinoso, F.; Kasuya, D.; Yudasaka, M.; Ijima, S. Cluster-Mediated Filling of Water Vapor in Intratube and Interstitial Nano spaces of Single-Wall Carbon Nanohorns. *Chem. Phys. Lett.* **2002**, *366*, 463–468.
43. Ohba, T.; Kanoh, H.; Kaneko, K. Affinity Transformation from Hydrophilicity to Hydrophobicity of Water Molecules on the Basis of Adsorption of Water in Graphitic Nanopores. *J. Am. Chem. Soc.* **2004**, *126*, 1560–1562.
44. Kimura, T.; Kanoh, H.; Kanda, T.; Ohkubo, T.; Hattori, Y.; Higaonna, Y.; Denoyel, R.; Kaneko, K. Cluster-Associated Filling of Water in Hydrophobic Carbon Micropores. *J. Phys. Chem. B* **2004**, *108*, 14043–14048.
45. Wier, K. A.; McCarthy, T. J. Condensation on Ultrahydrophobic Surfaces and Its Effect on Droplet Mobility: Ultrahydrophobic Surfaces Are Not Always Water Repellant. *Langmuir* **2006**, *22*, 2433–2436.
46. Narhe, R. D.; Beysens, D. A. Growth Dynamics of Water Drops on a Square-Pattern Rough Hydrophobic Surface. *Langmuir* **2007**, *23*, 6486–6489.
47. Cassie, A. B. D.; Baxter, S. Wettability of Porous Surfaces. *Trans. Faraday Soc.* **1944**, *40*, 546–551.
48. van Rijn, C. J. M. *Nano and Micro Engineered Membrane Technology*; Elsevier: Amsterdam, 2004.